Environmental Health Perspectives
Vol. 72, pp. 77-88, 1987

Ultrastructural Changes in the Nasal Mucosa of Fischer 344 Rats and B6C3F1 Mice Following an Acute Exposure to Methyl Isocyanate

by Linda C. Uraih,* Fred A. Talley,* Kunitoshi Mitsumori,* Bhola N. Gupta,* John R. Bucher,† and Gary A. Boorman*

Male rats and male mice received a single 2-hr exposure to 0 (control), 10, or 30 ppm of methyl isocyanate and were sacrificed after 1, 3, 14, or 90 days to assess the ultrastructural changes in the nasal mucosa by transmission electron microscopy. One day after exposure to methyl isocyanate, there were widespread areas of necrosis and degeneration of the respiratory and olfactory epithelium of rats and mice in the 10 ppm and 30 ppm groups. Qualitatively the ultrastructural findings were similar for both exposure groups and species. Degeneration followed by rapid regeneration was observed for both respiratory and olfactory epithelia but was most striking for olfactory epithelium in the dorsal meatus. Three days after the exposure, the olfactory epithelium was two to three cell layers thick due to a loss of supporting cells, olfactory neurons, and basal cells. By 14 days after exposure, the olfactory epithelium was composed of a heterogeneous cell population three to five cell layers thick. At 90 days following exposure, the epithelium was of normal thickness (eight to ten cell layers), with normal architectural arrangement, and composed of well-differentiated cells that appeared similar to those of controls. There were several findings that suggested the epithelial cells of Bowman's glands were the progenitor for the regenerating supporting cells of the olfactory epithelium. This study demonstrated that the respiratory and olfactory epithelium is capable of complete structural regeneration after an acute destruction by methyl isocyanate.

Introduction

Methyl isocyanate (MIC) is a reactive, toxic, and volatile liquid that is hazardous by all means of contact (*1*). In rodents, inhalation of MIC induces severe destruction of the mucosal linings of the upper (*2,3*) and lower (*2–4*) respiratory tracts. As assessed by light microscopy, the effects of MIC on the nasal mucosa were similar to those induced by other nasal toxicants such as chlorine (*5*), dimethylamine (*6*), and a number of other sensory irritants (*7*), which cause necrosis and erosion of the nasal respiratory and olfactory epithelia. Destruction of the mucosal lining of the nasal cavity inhibits mucociliary function (*8*) and olfaction (*9,10*). Although obvious degenerative changes may be observed by light microscopic examination, subtle pathological defects can be more fully appreciated ultrastructurally. The objective of this study was to examine and characterize ultrastructural changes in the nasal mucosa of rodents following an acute exposure to a toxic concentration of MIC.

*Chemical Pathology Branch, National Toxicology Program, P. O. Box 12233, Research Triangle Park, NC 27709.

†Carcinogenesis and Toxicology Evaluation Branch, National Toxicology Program, National Institute of Environmental Health Sciences, Research Triangle Park, NC 27709.

Materials and Methods

Male F344 rats and male B6C3F1 mice [source, animal care, disease surveillance, etc., detailed in a separate paper (*11*)] were sacrificed 1, 3, 14, and 90 days after a 2-hr whole-body exposure to 0, 10, or 30 ppm of MIC on 4/22/86. Details of exposure, generation, monitoring and safety have been reported (*12*). Each exposure group consisted of five rats/sex and five mice/sex. After a complete necropsy, the heads of two rats and two mice per group were removed and the nasal cavity was fixed by infusing Fowler's fixative, pH 7.4 (*13*), into the nasopharynx via syringe. The heads were then placed in 50 mL of fixative at 4°C and for no less than 5 days. After fixation and using Palatine structures as references (*14*), three transverse sections of the heads were made by using a Buehler's Isomet low speed saw. The following sections were taken: (1) through the incisive papilla and anterior to the first palatal ridge, (2) at the

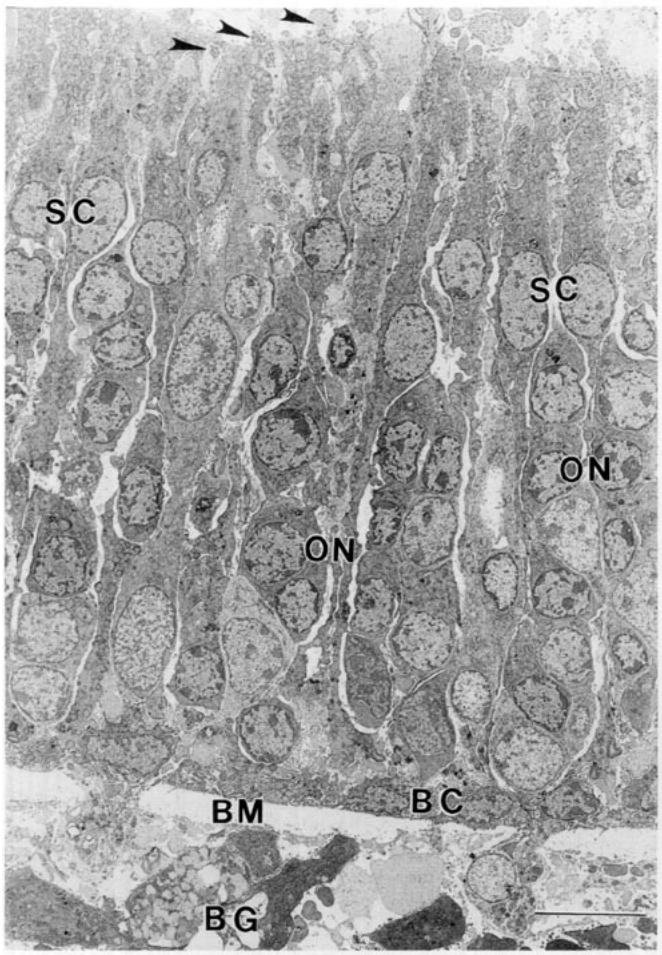

FIGURE 1. Rat, 0 ppm, 90 days. Electron micrograph of normal olfactory epithelium (8–10 cell layers). Olfactory dendritic vesicles (arrowwheads), supporting cells (SC), olfactory neurons (ON), basal cells (BC), basement membrane (BM), and Bowman's gland (BG). Bar = 10 μm.

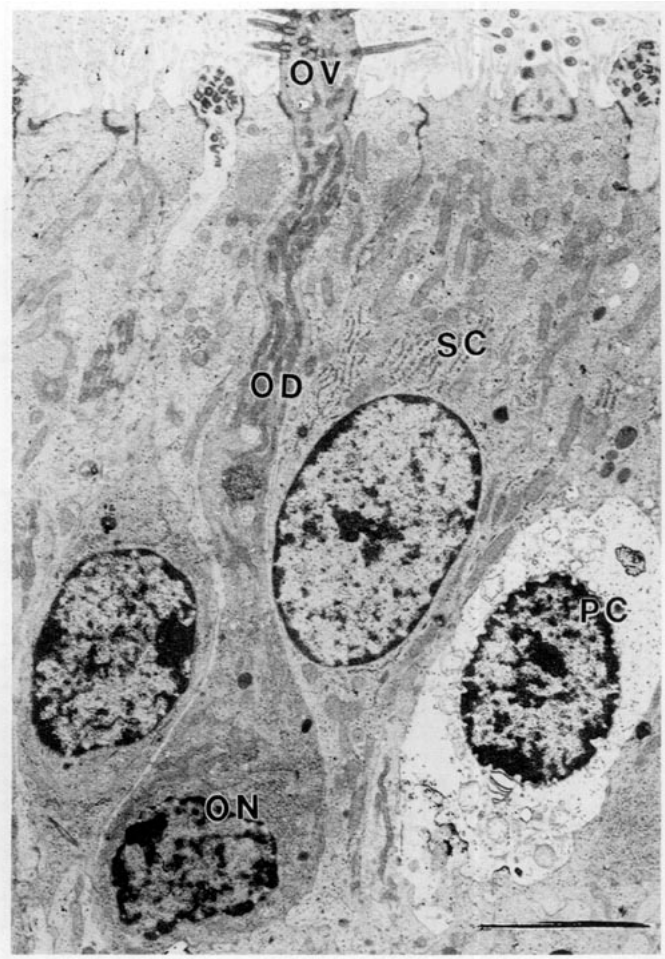

FIGURE 2. Rat, 0 ppm, 90 days. Normal olfactory neuron (ON), olfactory dendrite (OD), olfactory vesicle (OV) with ciliary extensions between two supporting (SC), pyknotic cell (PC) Bar = 5 μm.

second palatal ridge and (3) at the level of the first upper molar tooth. The sections were subsequently rinsed and placed in 0.2 M phosphate buffer (4°C). After 2 days, seven samples of the nasal mucosa were prepared for each animal by microdissection. At levels I and II, samples were taken from the respiratory epithelium of the septum and dorsal nasal conchae, and the olfactory epithelium from the dorsal meatus. At level III, a sample was taken from the olfactory epithelium of the dorsal meatus and ethmoid concha. These tissues were placed in fresh phosphate buffer overnight postfixed in 1% osmium tetroxide in 0.1 M phosphate buffer for 2 hr, dehydrated in graded concentrations of ethyl alcohol, infiltrated, and flat-embedded in Epon. Semithin sections (0.5–1 μm) were cut on a Sorvall MT-1 ultramicrotome and stained with toluidine blue for light microscopic evaluation. Ultrathin sections, stained in an LKB ultrastainer utilizing 0.5% uranyl acetate and 2.7% lead citrate, were examined in a Phillips 400 transmission electron microscope. Major attention was focused on the olfactory epithelium from the dorsal meatus at levels 2 and 3.

Results

Clinically, rats and mice in both exposure groups showed evidence of dypsnea and had ruffled hair coats. Unscheduled deaths occurred among mice and rats in the 30 ppm exposure group, and all rats in the 30 ppm dose group died before 90 days. A complete description of the in-life phase of this study is reported in another article in this volume (*11*).

Control animals had normal nasal mucosa. The respiratory and olfactory epithelium was similar for control rats and mice at each sacrifice interval. The respiratory epithelium from the nasal septum was composed of simple, ciliated columnar cells, goblet cells, and basal cells.

FIGURE 3. Rat, 10 ppm, 1 day. Complete destruction of respiratory epithelial layer in nasal septum accompanied by inflammatory cell infiltrates of neutrophilic leukocytes (N) and macrophages (M). Basement membrane (small arrowheads); degenerating epithelial cells (D); degradative products of epithelial cells (large arrowheads). Bar = 20 μm.

FIGURE 4. Rat, 10 ppm, 1 day. Axonal degeneration of olfactory nerve bundles in lamina propria. Axonal swelling (large arrowheads); degradation of axoplasm (small arrowheads); and accumulation of degradative products within Schwann cell processes (D). Bar = 25 μm.

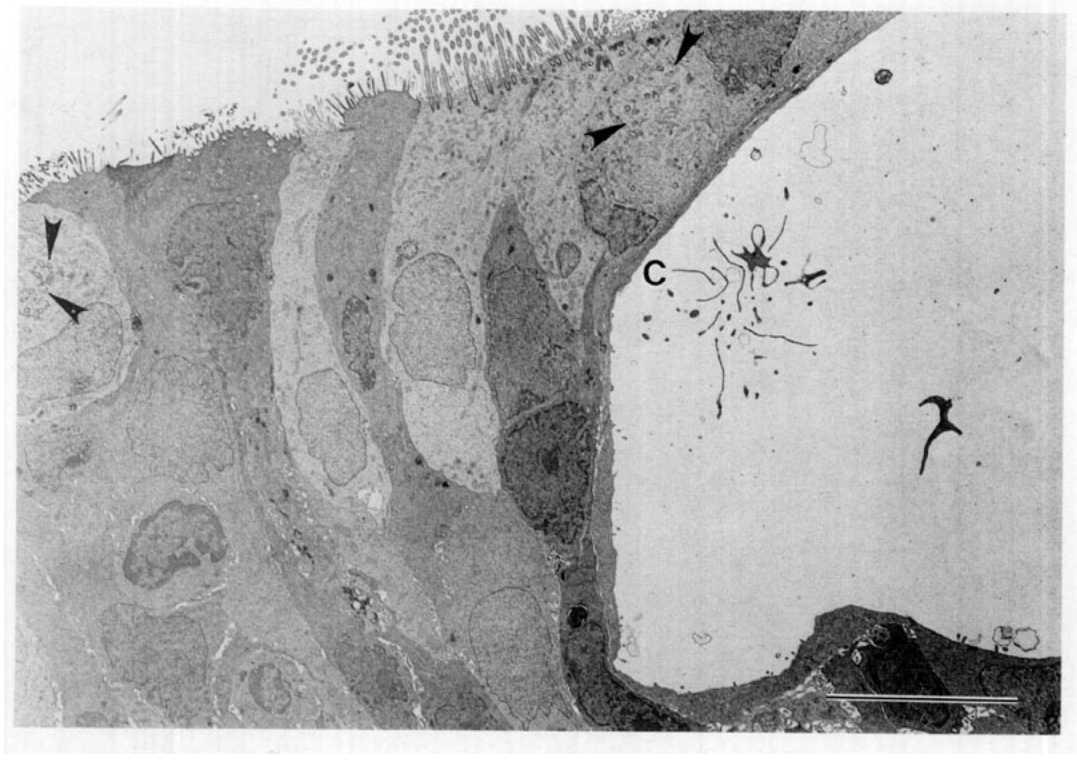

FIGURE 5. Rat, 10 ppm, 3 days. Intraepithelial cyst in dorsal nasal concha (C). Notice internalized cilia (arrows) within the cytoplasm of ciliated column cells. Bar = 10 μm.

Respiratory epithelium from the nasal concha was a pseudostratified columnar epithelium composed of ciliated cells, nonciliated columnar cells, goblet cells, cuboidal cells, brush cells, and basal cells. The lamina propria was composed of loose fibroelastic connective tissue, large venous plexuses, and mixed seromucous glands. Myelinated axons from the trigeminal nerve were especially prominent in section from the nasal septum. The olfactory epithelium taken from the dorsal meatus and the ethmoid turbinates was composed of three distinct cell types arranged in ill-defined layers giving a suggestion of an epithelium eight to ten cell layers thick (Fig. 1). The supporting cells (sustentacular cell) were tall columnar cells with a tapering base that attached to the basement membrane. The nuclei of supporting cells form the apical or superficial layer of the epithelium. These cells had numerous microvilli extending from their apical surface. The middle (six to seven cell layers) layers of the epithelium was composed of round nuclei of olfactory neurons arranged at different levels while maintaining a close association with one another. An apical dendritic process extended to the surface, alternating between the nuclei of supporting cells, and terminated into a club-shaped vesicle with ciliary extensions (Fig. 2). The third cell layer or basal cell layer was composed of small, round to spindle-shaped, electron-dense cells lying immediately above the basal lamina. The long cytoplasmic processes of these cells interdigitated with processes of neighboring cells or encompassed central processes of olfactory bipolar nerve cells. The lamina propria was composed of loose fibroelastic connective tissue, olfactory nerve bundles consisting of unmyelinated axons, and large venous plexuses. There were many large glands of Bowman which contained both serous and mucus producing cells. The cytoplasm of serous cells contained prominent profiles of concentrically arranged rough endoplasmic reticulum. The Bowman's gland and excretory duct could respectively be seen penetrating the basement membrane or within the olfactory epithelium.

One day after exposure to methyl isocyanate, there were random areas of degeneration and necrosis in the respiratory and olfactory epithelium in mice and rats. The most severely affected areas were characterized by necrosis of the entire epithelial cell lining with detachment of cells from the basement membrane and an acute inflammatory cell infiltrate in the epithelium and lamina propria (Fig. 3). Degeneration of olfactory nerve fibers and epithelial cells of Bowman's glands was also seen in the lamina propria. The degenerative changes of olfactory nerve fibers were characterized by swelling of axons, degeneration of mitochondria in axons, and degradation of axoplasm (Fig. 4). The severe change was seen at both exposure levels but covered greater areas in the 30 ppm exposure group. Less severe changes which could be seen within the same animal in variable

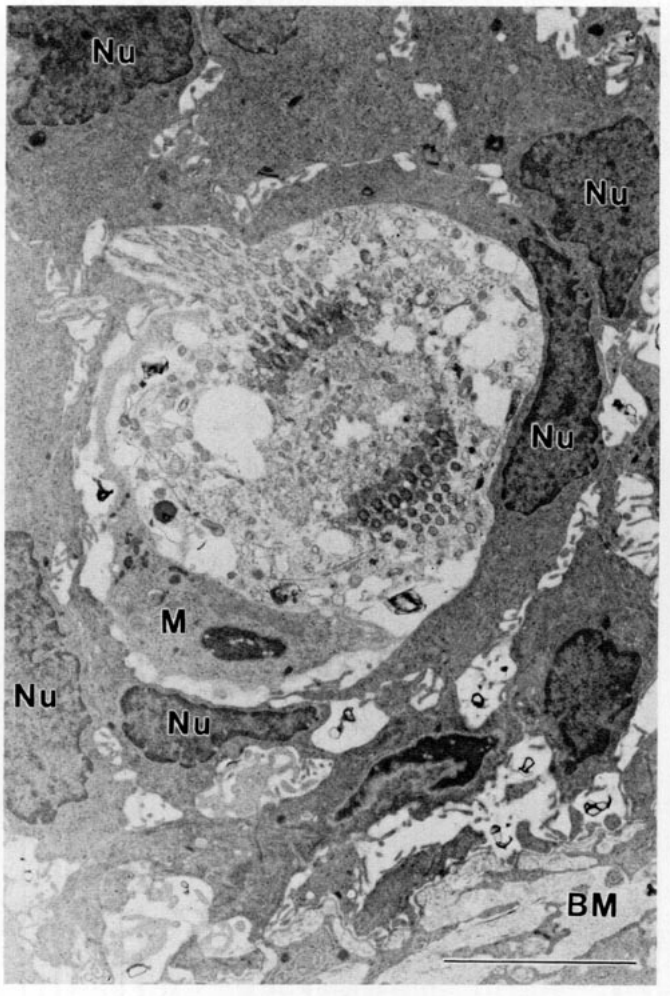

FIGURE 6. Rat, 10 ppm, 3 days. Phagocytosis of degenerated ciliated cells by macrophage (M) within an intraepithelial cyst of dorsal nasal concha. Nuclei of epithelial cells (Nu); basement membrane (BM). Bar = 5 μm.

regions were characterized by necrosis and degeneration of the superficial cell layers but basal cells remained viable. There were often no significant changes in nerve bundles or Bowman's glands in the lamina propria.

Three days after exposure to 10 or 30 ppm of MIC, the respiratory epithelium showed residual degenerative and inflammatory changes as well as regeneration. In the dorsal nasal concha, there was slight disorganization of the epithelium. Some ciliated cells showed clusters of internalized cilia in the cytoplasm (Fig. 5). In this area, large cystic spaces could occasionally be found within the epithelium. The changes were focal and varied among sections. Some sections showed long flattened surface cells with prominent intermediate filaments and tight cell junctions. Still other areas showed a minimal infiltration of phagocytic cells and mast cells within the epithelium and the lamina propria. Macrophages present in them contained phagocytized cilia and other cell debris (Fig. 6). There was an increased number of collagen fibers in the lamina propria and an ill-defined basement membrane. Similar but less severe changes were seen in the respiratory epithelium from the nasal septum. Regeneration of the respiratory epithelium at 3 days was characterized by a randomly arranged proliferation of immature epithelial cells. There was a wealth of free ribosomes and polysomes in the abundant cytoplasm of these cells. Endoplasmic reticulum and mitochondria could rarely be seen.

Three days after exposure, there was variation in the appearance of the olfactory epithelium from the dorsal meatus between levels II and III. At level II, the epithelium was often two cell layers thick and disorganized (Fig. 7). The epithelium contained flattened surface cells with sparse microvilli and prominent bundles of intermediate filaments, large round electron-lucent cells, and irregularly shaped but electron dense, subsurface cells which were poorly differentiated and lacked cell junctions. Olfactory vesicles were missing and there were no central nerve processes of olfactory bipolar neurons. In areas the excretory duct of Bowman's gland opened to the surface. This was often associated with cystic degeneration of the cells of Bowman's glands. In places, the cells of Bowman's glands almost totally formed the epithelium (Fig. 8). Olfactory nerve endings showed minimal degenerative changes which were similar to degenerative changes seen at 1 day past exposure. At level III of the dorsal meatus, fewer degenerative changes were found and there was more regeneration of the olfactory epithelium. The epithelium was at least three cell layers thick and the cells were slightly more organized with greater cell junctional relationship. The cell population was still heterogeneous, poorly differentiated, and mitotic figures were found. The predominant cell in this area was the large, round, electron-lucent cell with microvilli and dense secretory granules. There were occasional flattened surface cells with intermediate filaments and dense secretary granules (Fig. 9) similar to the epithelial cells of small acini of Bowman's glands. Irregularly shaped electron-dense cells lined the basal lamina and occasionally formed vertical columns, rows, or stacks leading from the basilar to the mid-apical region of the epithelium (Fig. 10). In the basal region, the cytoplasm of these cells encompassed the newly formed central nerve processes. A few olfactory vesicles with one or two ciliary extensions were present.

By day 14, the respiratory epithelium showed progressive regeneration with increased cell population and normal architecture. There were residual effects remaining in the most anterior levels of the dorsal nasal concha and nasal septum. Macromitochondria with bizarre configuration or reduplication of cristae was an infrequent finding (Fig. 11). In the high dose rats, the dorsal concha showed fewer ciliated cells and had a prepondrance of nonciliated columnar cells with rudimentary microvilli. There was no secretory activity. The

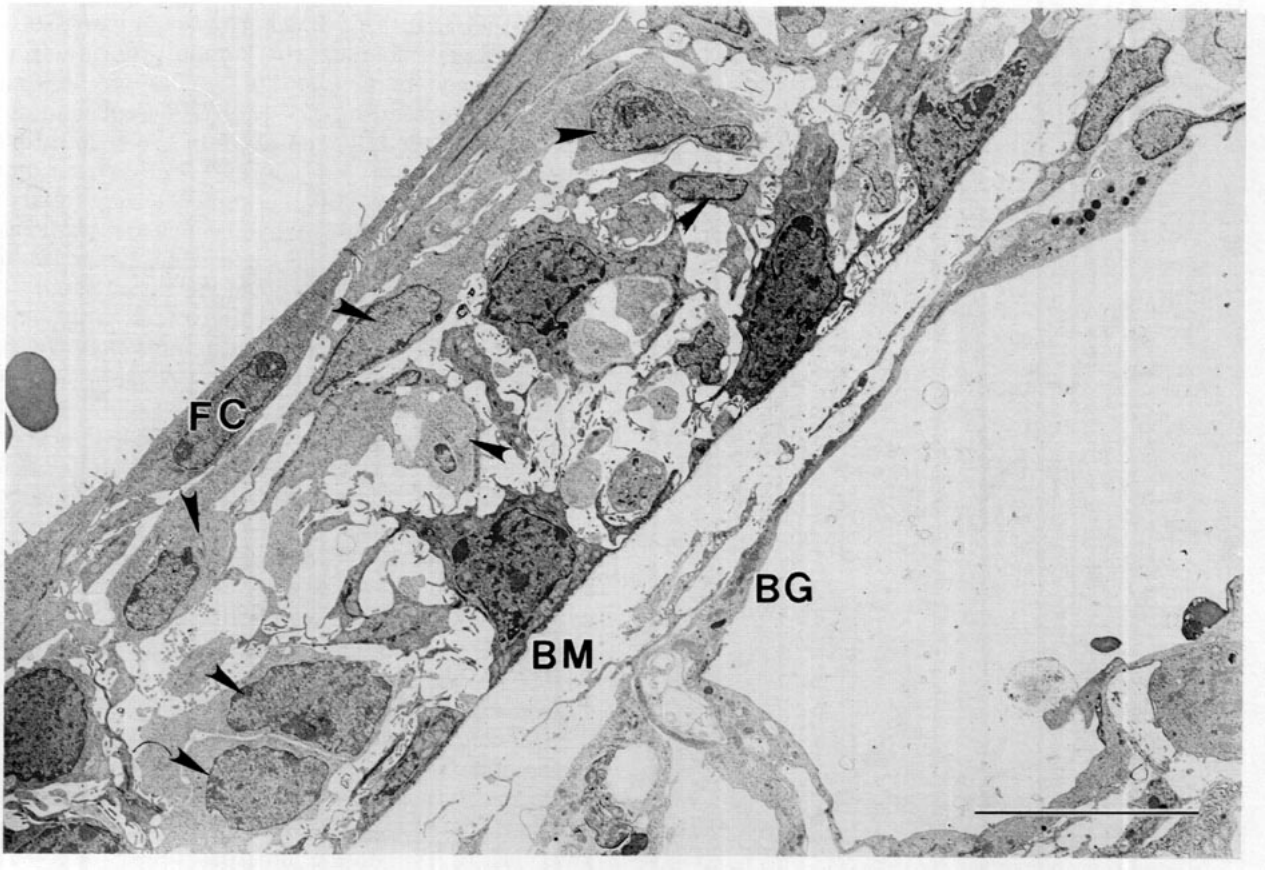

FIGURE 7. Rat, 10 ppm, 3 days. Olfactory epithelium reduced to two to three cell layers and lacked dendritic vesicles, olfactory neurons, and nerve bundles. Abnormal, flattened cell (FC) on surface, poorly differentiated cells (arrowheads), basement membrane (BM), and cystic dilatation of Bowman's gland (BG). Bar = 10 μm.

basement membrane in this area was ill-defined or irregular.

The olfactory epithelium, after 14 days, showed evidence of progressive regeneration. The epithelium was three to five cell layers in thickness and composed of regenerating supporting cells, olfactory neurons and basal cells. Respiratory metaplasia characterized by columnar ciliated cells was seen between regenerating supporting cells of the olfactory epithelium (Fig. 12). Olfactory vesicles with two to three ciliary extensions were occasionally seen but most were rudimentary vesicles seen intraepithelialarly, migrating toward the surface or above the surface but lacking in ciliary extensions (Fig. 13).

At 90 days after the exposure to MIC, the respiratory epithelium showed complete and orderly re-epithelialization of the dorsal nasal concha and nasal septum in the sections examined. Ultrastructural alterations in cilia and nerve fibers were not found.

Although an area of respiratory metaplasia in the ethmoid turbinate was still evident 90 days after exposure, there appeared to be complete structural regeneration of the olfactory epithelium in the dorsal meatus. The epithelium was eight to ten cell layers thick (Fig. 14). The morphology of the supporting cells was similar to the epithelial cells of Bowman's glands. The cytoplasm of supporting cells occasionally showed lamellar agranular endoplasmic reticulum which were prominent in the cytoplasm of epithelial cells of Bowman's glands after 14 days. The olfactory neurons could be positively identified at this time by the prominent golgi apparatus usually in the apical portion of the cytoplasm (Fig. 15). Olfactory vesicles were present with normal ciliary extensions. The basal cells were in alignment along the basement membrane and the cytoplasm showed the normal intimate contact with regular proliferations of small nerve bundles. The basement membrane was well defined except for areas where cells of Bowman's glands extended through the basement membrane (Fig. 16). In this same area, acini of Bowman's glands within the olfactory epithelium were lined by large round immature cells similar to supporting cells seen previously at 14 days, while the cells of Bowman's glands beneath the basement membrane were characterized by the prominent lamellar agranular endoplasmic reticulum and secretory granules. The lamina

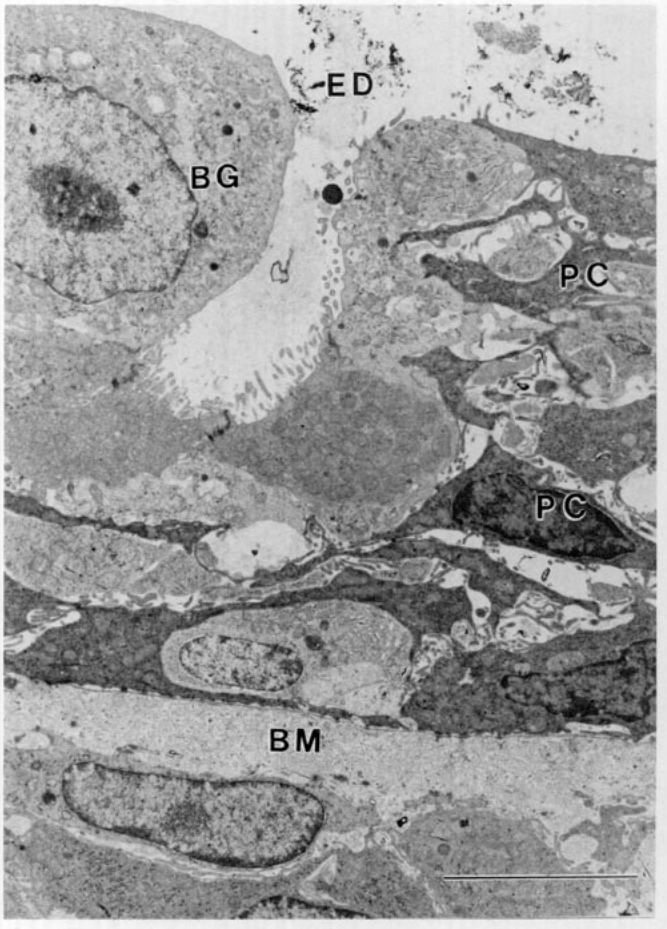

FIGURE 8. Rat, 30 ppm, 3 days. Dorsal meatus at level II where olfactory epithelium is almost totally occupied by Bowman's gland (BG). Notice microvillate excretory duct open to surface (ED); heterogeneous poorly differentiated cells with many cell processes (PC) and basement membrane (BM). Bar = 5 μm.

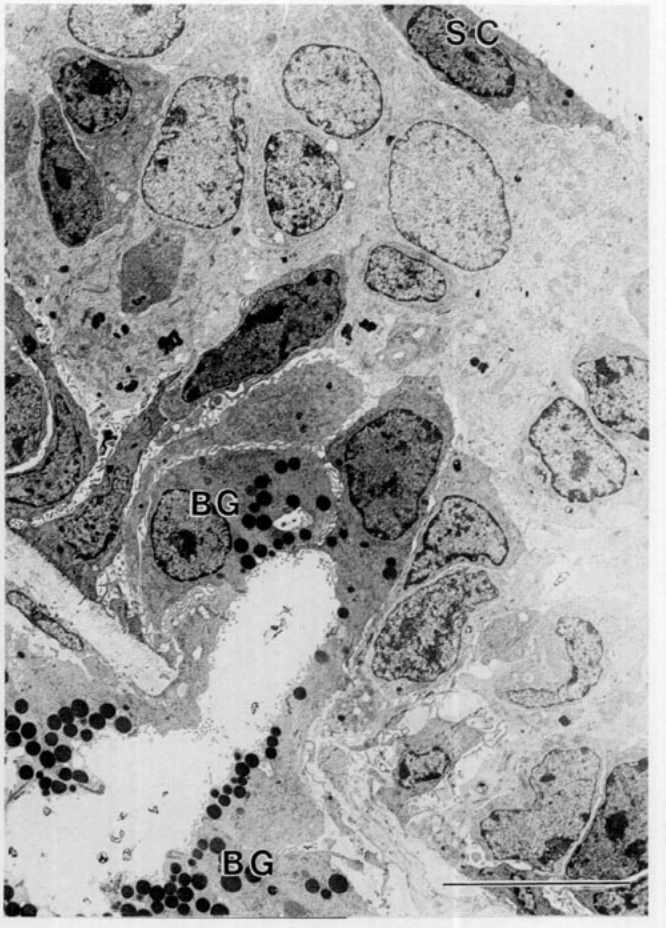

FIGURE 9. Rat, 10 ppm, 3 days. Squamous metaplasia in olfactory epithelium from dorsal meatus. Notice flattened surface cell with bundles of intermediate filament and dense secretory granules (SC) similar to epithelial cells of Bowman's gland (BG) protruding through basement membrane. Bar = 10 μm.

propria was composed of normal olfactory unmyelinated axons, Bowman's glands, and vasculature.

Discussion

Methyl isocyanate exposure caused necrosis, cellular degeneration, and detachment of the cells from the basement membrane both in the respiratory and olfactory epithelia of the nasal mucosa. The degenerative changes in the nasal mucosa were random in occurrences and appeared to be nonspecific responses of the cells to injury. Similar degenerative findings in the olfactory epithelium were seen in mice 24 hr after nasal irrigation with zinc sulfate (a compound known to selectively damage olfactory epithelium) (*15*). Internalized cilia were seen in this study as well as in rats after an acute exposure to formaldehyde (*16*) and in hamsters after mechanical injury to the trachea (*17*). In this study, this finding was considered a state of ciliogenesis since the associated cells showed active regeneration. The intraepithelial cyst and active phagocytosis of degenerated cells seen in this study could not be found mentioned in the literature. The macromitochondria with reduplication of cristae were nonspecific intracellular responses to injury and may represent an enzyme deficiency or suppression of mitochondrial division (*18*). The flattened surface cells in the respiratory olfactory epithelium was likely an early squamous metaplasia since there were dense bundles of intermediate filaments similar to tonofilaments. Squamous metaplasia and respiratory metaplasia have been reported in a variety of studies of known nasal inhalants (*6,7,16*). However, squamous metaplasia was not seen during the light microscopic examination of the nasal epithelium of mice after an acute exposure with MIC (*2*).

The olfactory epithelium is highly sensitive to toxic gases (*5*). The loss of supporting cells, sensory cells, basal cells and olfactory nerves were most obvious in level II of the dorsal meatus in this ultrastructural study. This finding has been seen at the light microscopy

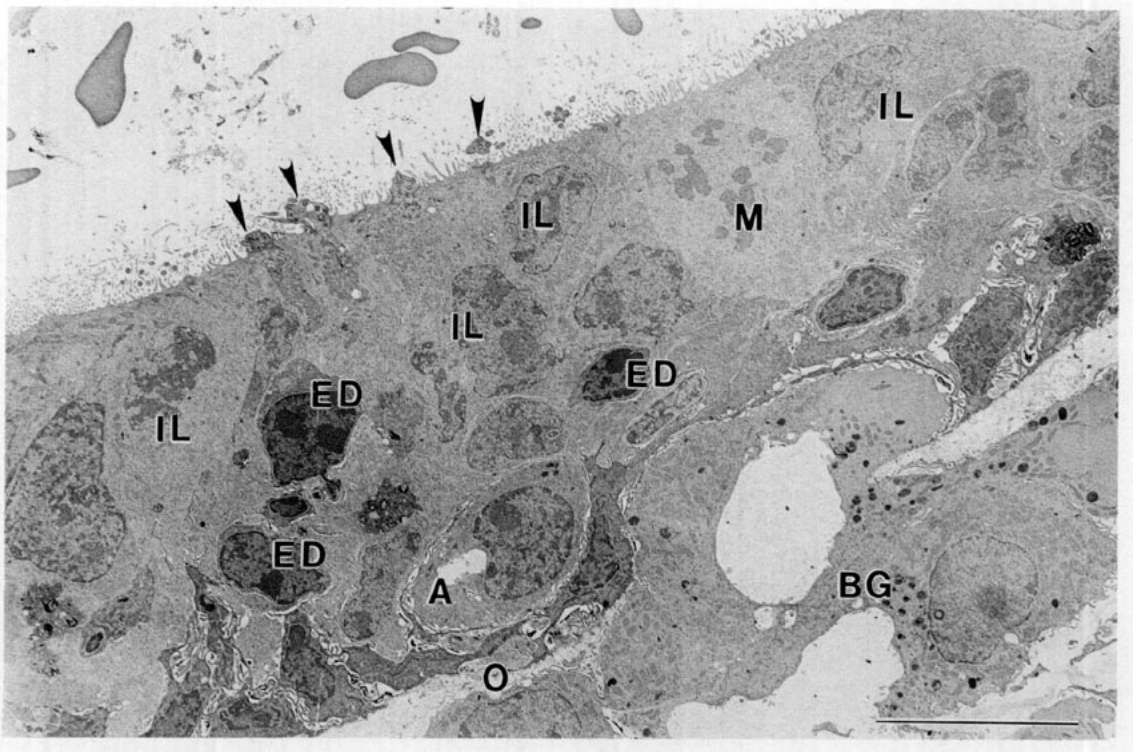

FIGURE 10. Mouse, 30 ppm, 3 days. Olfactory epithelium in early regenerative phase. Note mitosis in epithelial cell (M); few olfactory vesicles (large arrowheads); acini of Bowman's gland (A) among epithelial cells; randomly arranged large electron lucent cells (IL) and electron dense cells (ED) lining the basal lamina and in vertical rows; regenerated olfactory nerves (O). Bar = 10 μm.

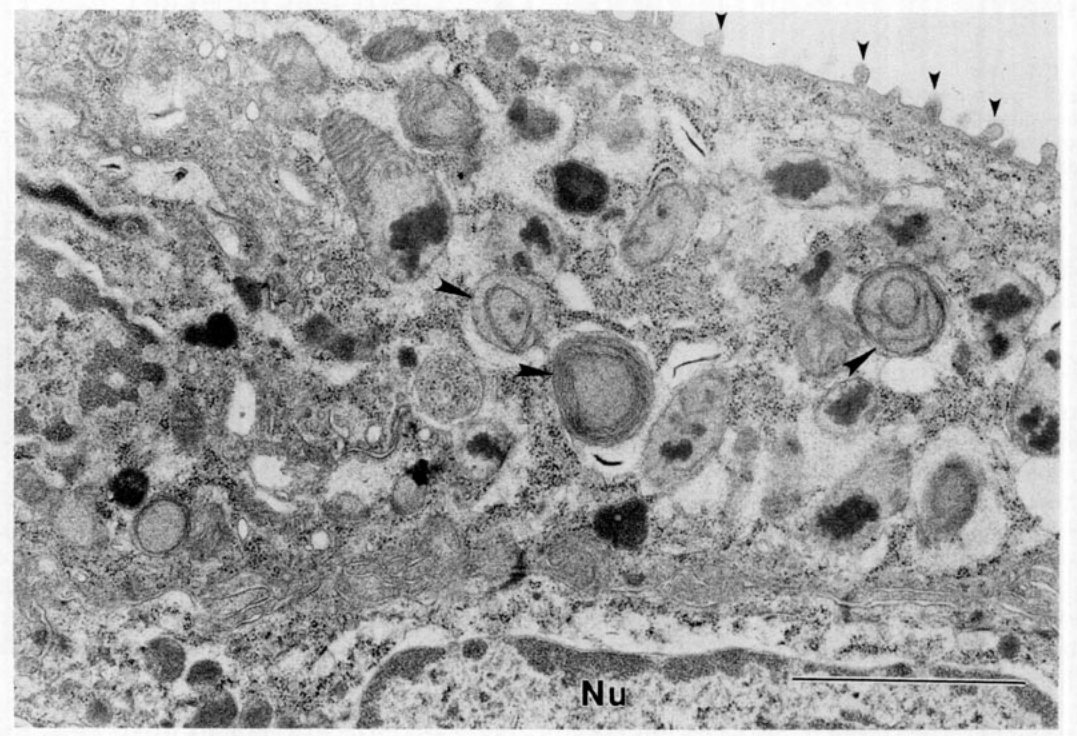

FIGURE 11. Mouse, 10 ppm, 14 days. Intracellular degeneration in nonciliated cuboidal cell from the dorsal nasal concha. Notice macromitochondria with reduplication of cristae (large arrowheads), electron dense accumulations in matrix region of mitochondria; nucleus (Nu) and microvilli (small arrowheads). Bar = 2 μm.

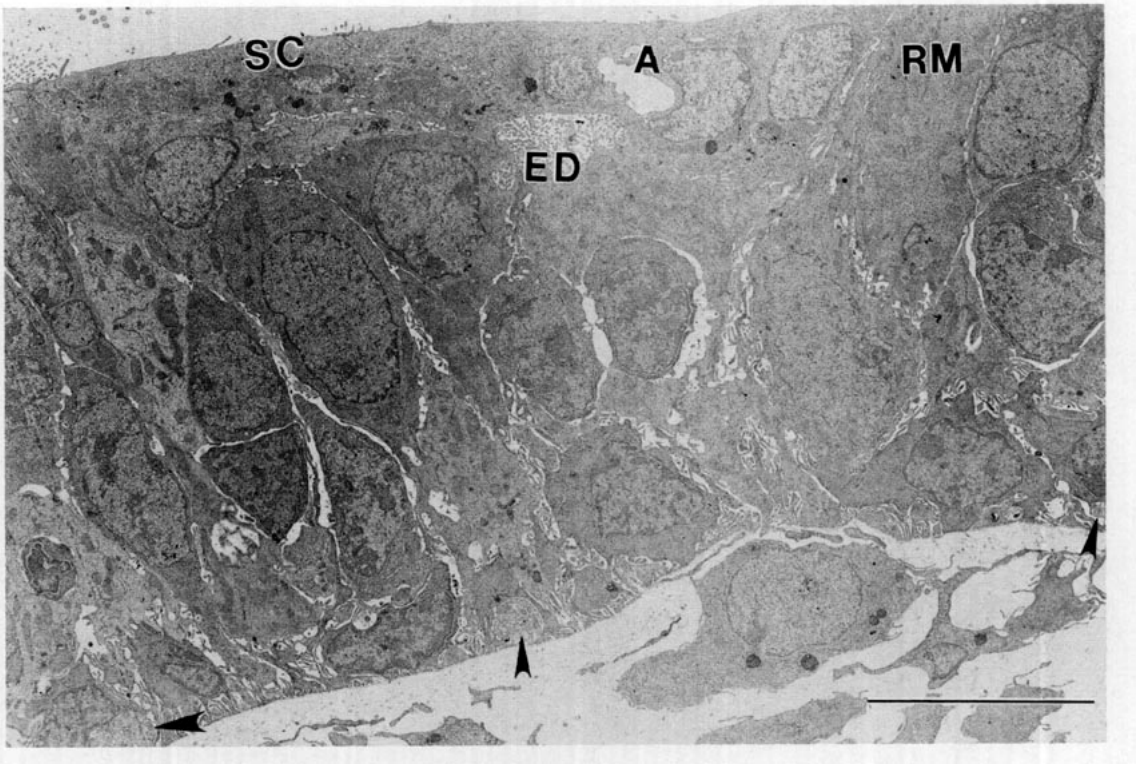

FIGURE 12. Mouse, 30 ppm, 14 days. Olfactory epithelium three to five cell layers thick. Notice flattened surface cell with dense secretory granules (SC), excretory duct of Bowman's gland (ED), acini formation (A), respiratory metaplasia (RM), and regenerated axons (arrowheads). Bar = 10 μm.

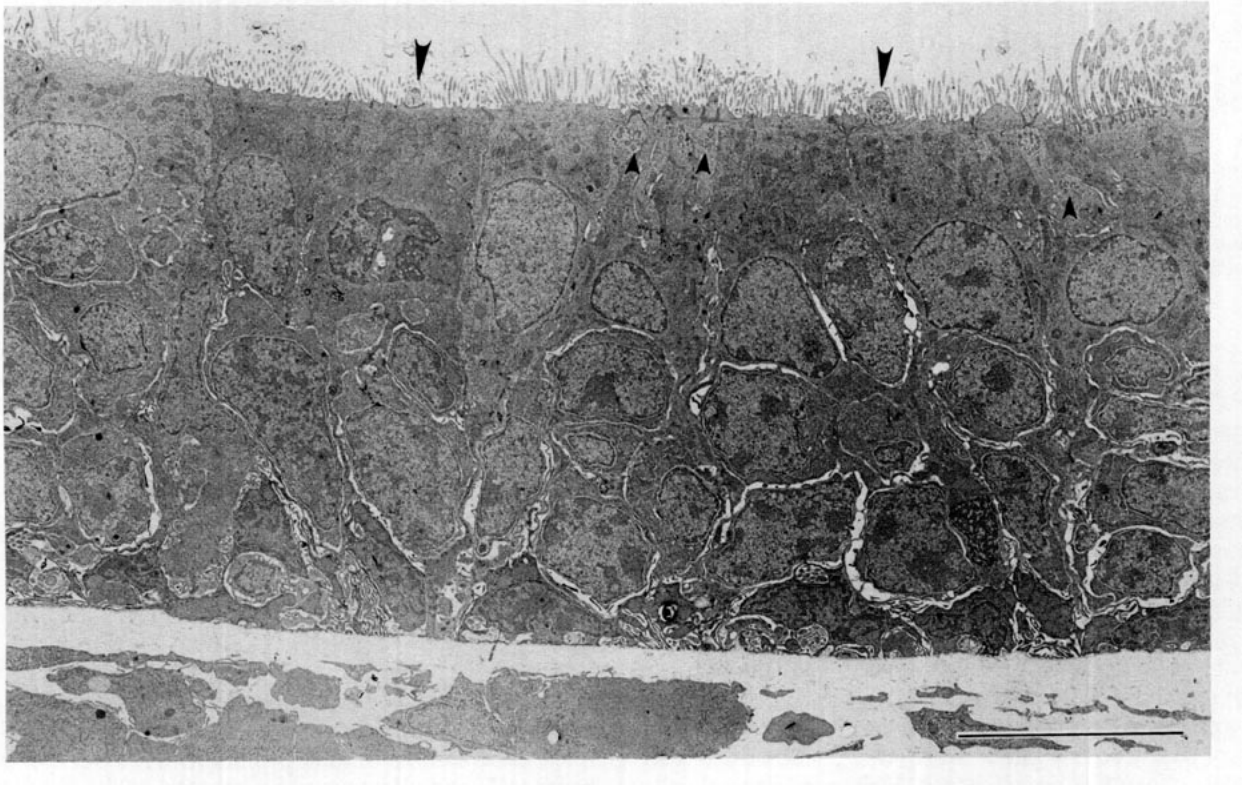

FIGURE 13. Mouse, 30 ppm, 14 days. Olfactory dendritic vesicles are fewer in number and lack ciliary extension (large arrowheads). Note rudimentary vesicles migrating toward the surface (small arrowheads). Bar = 10 μm.

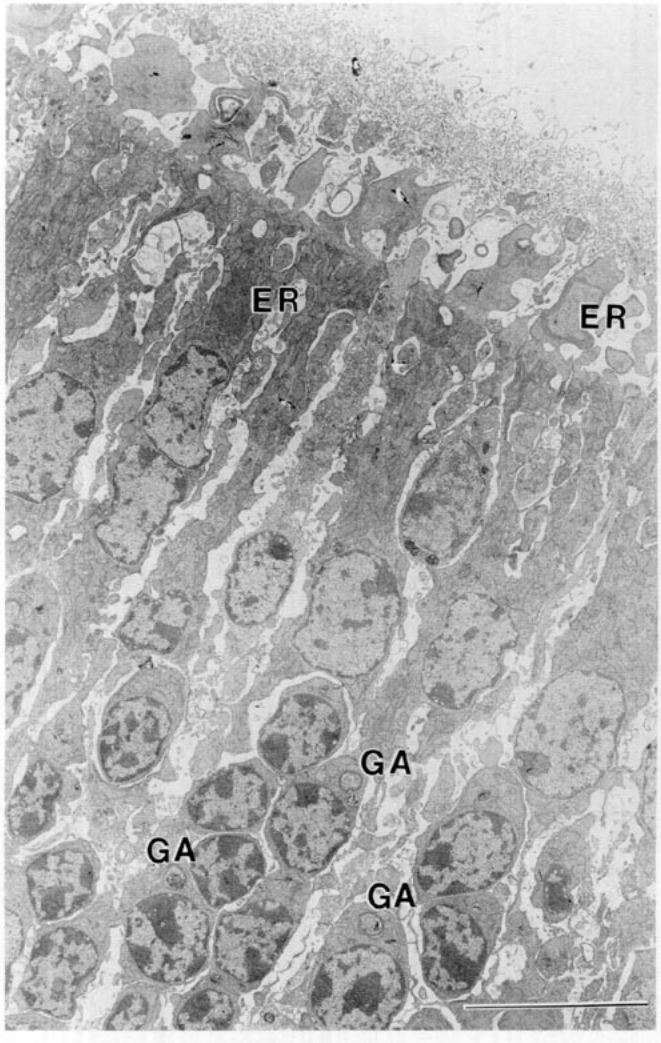

FIGURE 14. Rat, 10 ppm, 90 days. Regeneration of olfactory epithelium (8–10 cell layers thick) similar to control. Cytoplasm of supporting cells contains laminated agranular endoplasmic reticulum (ER). Notice prominent golgi apparatus (GA) in the apical portion of olfactory neuron. Bar = 10 μm.

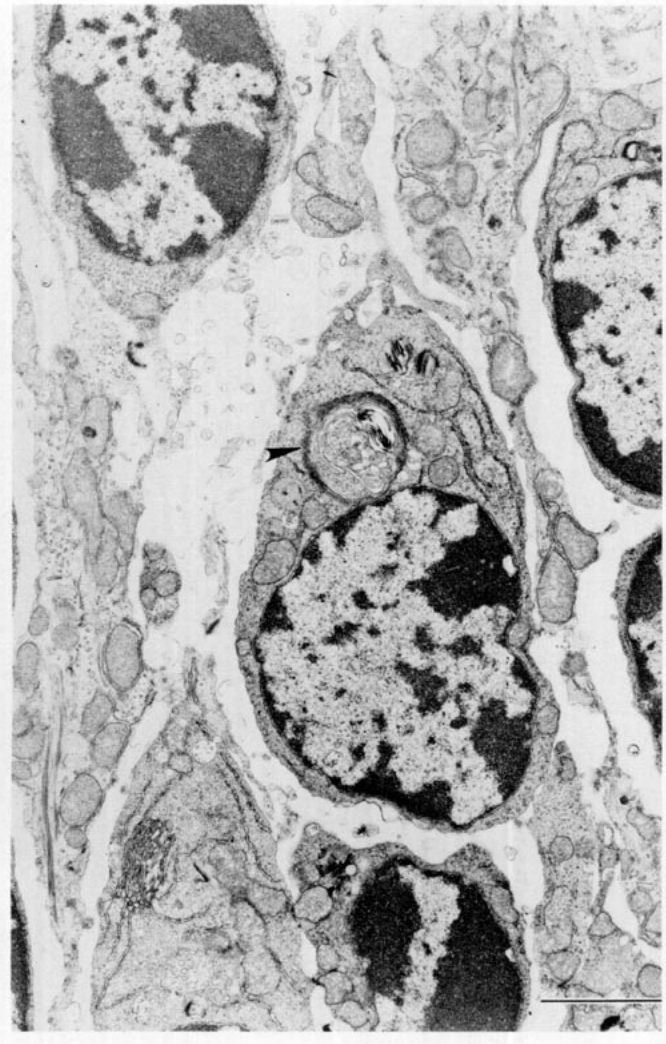

FIGURE 15. Mouse, 0 ppm, 90 days. Olfactory neuron with prominent golgi apparatus (arrowhead) usually in apical portion of cell. Bar = 2 μm.

level during the studies of several nasal toxicants in mice (*7*), rats (*6*), and hamsters (*19*), and had a similar ultrastructural appearance to mice treated with zinc sulfate (*15*). The most striking finding in this study was the rapidity with which the respiratory and olfactory epithelium regenerated. Three days after exposure to toxic concentrations (10–30 ppm) of MIC early regeneration was evident in the nasal cavity and was basically complete by 90 days. There are several studies in mice (*15,20–22*), in frog (*23*), and in fish (*24*) that show the regenerating capability of the olfactory epithelium. In early stages of regeneration, the olfactory epithelum was approximately two to three cell layers thick, and cells of Bowman's glands were the predominant cell type. As the epithelium became thicker, additional cells began to proliferate with an architectural arrangement and morphologic features of the normal epithelium (*25*). After 14 days, Bowman's glands within the epithelium were lined by immaturelike large round cells similar to regenerating supporting cells, while in the laminar propria the glands were mature and active and filled with agranular endoplasmic reticulum. Supporting cells could occasionally be seen with secretory granules and lamellar agranular endoplasmic reticulum similar to that seen in epithelial cells of Bowman's glands. These findings were in agreement with those reported for mice after treatment with zinc sulfate (*20*) and suggest that the epithelial cells of Bowman's glands are the progenitor for the supporting cells. Some morphologic similarities, i.e., electron-dense cells arranged vertically from nasal lamina of midepithelium were seen between basal cells and olfactory neurons. Autoradiographic and morphological observations in mice have identified the

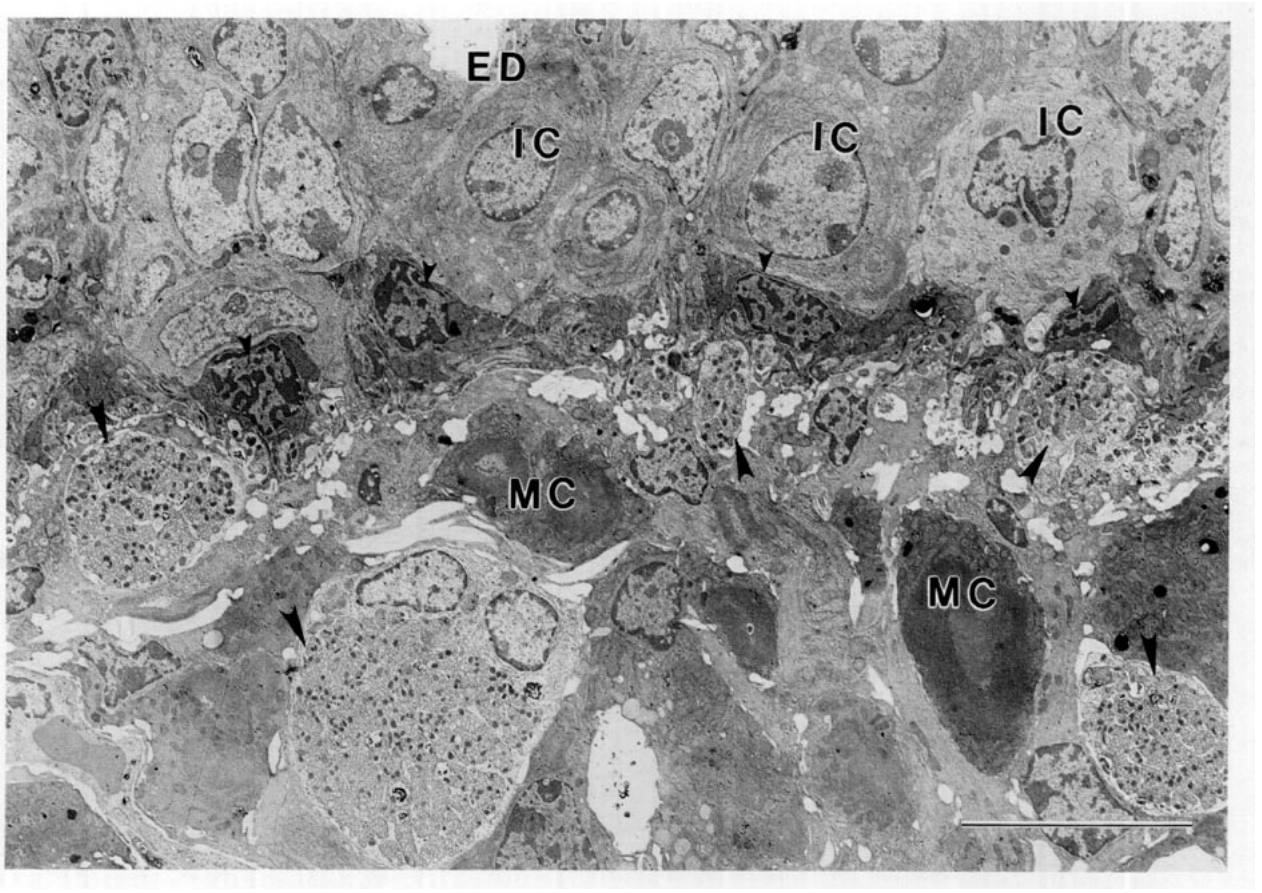

FIGURE 16. Mouse, 30 ppm, 90 days. An area in the basilar region of the olfactory epithelium from the dorsal meatus. Notice large, round, immature cells lining Bowman's glands within the epithelium (IC) and more mature-appearing cells with agranular endoplasmic reticulum of Bowman's gland beneath the basement membrane (MC); excretory duct of Bowman's gland (ED); basal cells (small arrowheads); olfactory unmelinated nerve fibers (large arrowheads). Bar = 10 μm.

basal cell as the stem cell of the olfactory neuron (*21–23*).

There were changes such as early mild squamous metaplasia and cilia defect which can best be described at the ultrastructural level or may not be obvious at the light microscopy level. A better characterization of the cell dynamics and some suggestions as to the progenitor of the repopulating cells can be made from this ultrastructural review.

The authors are grateful to John Horton for his technical assistance in preparing and sectioning the tissues. We also thank Delores York and Phyllis Duff for typing the manuscript.

REFERENCES

1. Union Carbide Corp. Union Carbide Handbook: Methyl Isocyanate. Union Carbide Corp., NY, 1976, pp. 15–25.
2. Boorman, G. A., Uraih, L. C., Gupta, B. N., Brown, R., and Bucher, J. R. Acute methyl isocyanate inhalation and recovery study in B6C3F1 mice. Toxicol. Appl. Pharmacol., in press.
3. Bucher, J. R., Boorman, G. A., Gupta, B. N., Uraih, L. C., Hall, L. B., and Stefanski, S.A. Two-hour methyl isocyanate inhalation exposure and 91-day recovery: a preliminary description of pathologic changes in F344 rats. Environ. Health Perspect. 72: 71-75 (1987).
4. Nemery, B., Densdale, D., Sparrow, A., and Ray, D. E. Effects of methyl isocyanate on the respiratory tract of rats. Brit. J. Ind. Med. 42: 799–805 (1985).
5. Jaing, X. Z., Buckley, L. A., and Morgan, K. T. Pathology of toxic responses to the RD50 concentration of chlorine gas in the nasal passages of rats and mice. Toxicol. Appl. Pharmacol. 71: 225–236 (1983).
6. Buckley, L. A., Morgan, K. T., Swenberg, J. A., James, R. A., Ham, T. E., Jr., and Barrow, C. S. The toxicity of dimethylamine in F-344 rats and B6C3F1 mice following a 1-year inhalation exposure. Fund. Appl. Toxicol. 5: 341–352 (1985).
7. Buckley, L. A., Jiang, Y. Z., James, R. A., Morgan, K. T., and Barrow, C. I. Respiratory tract lesions induced by sensory irritants at the RD50 concentration. Toxicol. Appl. Pharmacol. 74: 417–429 (1984).
8. Morgan, K. T., Patterson, D. L., and Gross E. A. Responses of the nasal mucociliary apparatus of F344 rats to formaldehyde gas. Toxicol. Appl. Pharmacol. 82: 1–13 (1986).
9. Naus, A. Alterations of the smell acuity caused by methol. J. Laryngol. 82: 1009–1011 (1968).
10. Adams, R. G., and Crabtree, N. Anosmia in alkaline battery workers. Brit. J. Ind. Med. 18: 216–221 (1961).
11. Bucher, J. R., Gupta, B. N., Adkins, B. A., Jr., Thompson, M., Jameson, C. W., Thigpen, J. E., and Schwetz, B. A. The toxicity

of inhaled methyl isocyanate in F344/N rats and B6C3F1 mice. I. Acute exposure and recovery studies. Environ. Health Perspect. 72: 53–61 (1987).
12. Adkins, B. Jr., O'Connor, R., and Dement, J. Inhalation exposure system used for acute and repeated-dose methyl isocyanate exposures of laboratory animals. Environ. Health Perspect. 72: 45–51 (1987).
13. Fowler, B. A., Kardish, R. M., and Woods, J. S. Alteration of hepatic microsomal structure and function by indium chloride. Lab. Invest. 48: 471–478 (1983).
14. Young, J. T. Histopathologic examination of the rat nasal passages: preparation and morphological features. In: Toxicology of the Nasal Passages (C. S. Barrow, Ed.), Hemisphere Pub. Co., Washington, DC, 1981, pp. 27–36.
15. Matulionis, D. H. Light and electron microscopic study of the degeneration and early regeneration of olfactory epithelium in the mouse. Am. J. Anat. 145: 79–100 (1975).
16. Montiero-Rivere, N. A., and Popp, J. A. Ultrastructural evaluation of acute nasal toxicity in the rat respiratory epithelium in response to formaldehyde gas. Fund. Appl. Toxicol. 6: 251–252 (1986).
17. McDowell, E. M., Becci, P. J., Schurch, W., and Trump, B. F. The respiratory epithelium. VIII. Epidermoid metaplasia of hamster tracheal epithelium during regeneration following mechanocal injury. J. Natl. Cancer Inst. 62: 995–1008 (1979).
18. Cheville, N. F. Pathologic Mitochondria in Cell Pathology, 2nd ed. Iowa State University Press, Ames, IA, 1983, pp. 118–121.
19. Feron, V. J., and Kruysse, A. Effects of exposure to furfural vapour in hamsters simultaneously treated with benzo(a)pyrene or diethylnitrosamine. Toxicology 11: 127–144 (1978).
20. Matulionis, D. H. Ultrastructural study of mouse olfactory epithelium following destruction by $ZnSO_4$ and its subsequent regeneration. Am. J. Anat. 142: 67–90 (1976).
21. Moulton, D. G. cell renewal in the olfactory epithelium. In: Olfaction and Taste, Vol. V (D. A. Denton and J. P. Coghlan, Eds.), Academic Press, New York, 1975, pp. 111–114.
22. Graziadei, P. P. C., and Graziadei, G. A. M. Neurogenesis and neuron regeneration in the olfactory system of mammals. I. Morphological aspects of differentiation and structural organization of the olfactory sensory neurons. J. Neurocytol. 8: 1–18 (1979).
23. Graziadei, P. P. C. Cell dynamics in the olfactory mucosa. Tissue Cell 5: 113–131 (1973).
24. Cancalon, P. Degeneration and regeneration of olfactory cells induced by $ZnSO_4$ and other chemicals. Tissue Cell 14: 717–733 (1982).
25. Frisch, D. Ultrastructure of mouse olfactory mucosa. Am. J. Anat. 121: 87–120 (1967).